Key Engineering Materials
ISSN: 1662-9795, Vol. 395, pp 209-232
doi:10.4028/www.scientific.net/KEM.395.209

Online: 2008-10-21

"Vapour Phase preparation and characterisation of SiC_f-SiC and C_f-SiC ceramic matrix composites"

A.Udayakumar[1, a], R.Bhuvana[1, b], S. Kalyanasundaram[2, c], Dr. J.Subrahmanyam[3, d], Dr.M.Balasubramanian[4, e], Dr. T.S.Kannan[1, f]

[1]Materials Science Division, National Aerospace Laboratories, Post Bag No. 1779, Bangalore-560017

[2]Structural Technologies Division, National Aerospace Laboratories, Post Bag No. 1779, Bangalore-560017

[3]Head, Composites Division, DMRL, Hyderabad

[4]Associate professor, Comp-Tec center, Indian Institute of Technology, Madras, Chennai-600036.

[a]audayk@yahoo.com, [b]bhuvana_mct@yahoo.com, [c]kalyan@css.nal.res.in, [d]jsm@dmrl.ernet.in, [e]mbala@iitm.ac.in, [f]kannants@lycos.com

Keywords: Ceramic Matrix Composites, Chemical Vapour Infiltration, Chemical Vapour Deposition, Interface, SiC_f-SiC composites, Nicalon CG Cloth, Methyl Trichloro Silane (MTS).

Abstract:

Several 2D SiC_f-SiC and C_f-SiC composites were fabricated using isothermal and isobaric Chemical Vapour Infiltration (ICVI) process. The reinforcements used in the above composites are Nicalon CG fabric and C fabric. Prior to SiC matrix infiltration, BN and C interfaces were applied to the fibre by using the pre-cursors Boron Trichloride (BCl_3)-Ammonia (NH_3) and Methane (CH_4) respectively to improve the mechanical performance of the composites. SiC matrix was infiltrated by the decomposition of Methyl Trichloro Silane-CH_3SiCl_3 (MTS) in the presence of hydrogen at the temperature ranging from 950°C to 980°C. H_2/MTS flow rate ratio used for this study is 16:1.An appropriate temperature for uniform SiC infiltration without any premature pore closures have been obtained by kinetic experiment. Density and porosity of the above composites were measured using the method described by EN1389:2003. Various mechanical characterizations like flexural strength, tensile strength and fracture toughness of the SiC_f-SiC composites were also studied. The SiC_f-SiC composites were subjected to thermal exposure (1000°C for 100 hr in an oxidizing atmosphere) and tensile strength results obtained before and after thermal exposure were compared. RT Flexural Strength and Fracture Toughness (K_{IC}) of composite-SQAV (SiC_f/C/SiC) and composite-SQBII (SiC_f/BN/SiC) are measured by 3-point bending and results were compared. RT Flexural strength of C_f-SiC composites with C interface of two thicknesses were measured and

compared. X-ray diffraction and microstructure studies have been made to confirm the β-SiC and to see the fibre/matrix interface, uniformity of infiltration, fibre pullout and crack deflections.

1. Introduction

Advanced next generation engines of aircraft and space vehicle need better materials to have an increased thrust-to-weight ratio with higher safety, reliability and reduced life cycle cost. To achieve these goals, novel or advanced materials are required. Continuous Fibre reinforced Ceramic Matrix Composites (CFCCs) are materials that are receiving a great deal of attention in this regard. CFCCs are the leading candidate materials for a number of applications in turbine engines for aircraft, future space vehicles (re-usable launch vehicles, space operation vehicles, etc) and land based power generation systems. CFCCs are being developed for use in high temperature structural applications because of their improved flaw tolerance, large work of fracture and non-catastrophic failure [1, 2]

Silicon Carbide fibre reinforced Silicon Carbide ceramic matrix composites (SiC_f-SiC**)** and Carbon fibre reinforced Silicon Carbide ceramic matrix composites (C_f-SiC) are better candidate materials because of their lower density, high temperature strength, fracture toughness (>20MPa√m), corrosion and erosion resistance. Chemical Vapour Infiltration (CVI) is the variant of Chemical Vapour Deposition (CVD) process used to manufacture various refractory matrix materials (e.g. SiC, C, Si_3N_4, B_4C, BN, etc) of fibre reinforced ceramic composites. During CVI process, the gaseous precursors are allowed to diffuse and infiltrate the fibrous porous structure (preform) and react at high temperature and atmospheric or low pressure to deposit a solid refractory material on the surface of the fibre in the preform. The by-products and un-reacted reactants are driven out of the fibre performs unlike in the CVD process. Though CVI and CVD have the same thermodynamics and chemistry, their kinetics are different. In CVI process, the processing conditions are tailored such that the deposition process occurs in the kinetically limited low temperature regime to obtain maximum uniform infiltration and densification of the composites [3]. The CVI process was developed in 1962 to densify porous graphite preform by infiltration with carbon matrix [4]. CVI, which is a vapour phase fabrication type, has unique characteristics such as good throwing power, the ability to deposit refractory materials at temperatures far below the normal ceramic processing (e.g. hot pressing, hot isostatic pressing and shaping followed by sintering, etc.) temperatures, and the capability of producing materials of exceptionally high purity with improved mechanical properties. Since the temperature and pressure involved in CVI process are not very high, there are very little thermal, chemical or mechanical damages to the reinforcement as compared to the conventional densification and the hot pressing methods. There are several review articles on CVD/CVI [5-7].

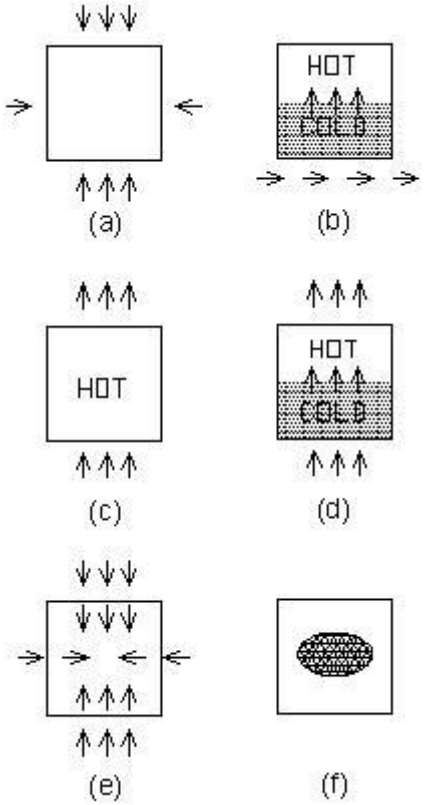

a: ICVI- Reagents surround Preform and enter via diffusion. (Conventional CVI : ICVI)

b: TGCVI- Reagents contact cold surface of Preform and enter via diffusion.

c: FCVI- Reagents flow through Preform

d: **TGFCVI-** Reagents flow through preform from cold to hot surface. (Forced CVI : FCVI)

e: PCVI- Reagents flow into and out of Preform because of cyclical evacuation and backfilling.

f: **MWCVI-** Reagents enter Preform via diffusion. Densification occurs from inside out. (Avoids interruption of the process in CVI to machine the skin of the component being densified)

Fig .1 Types of CVI processes

There are various types of CVI processes as shown fig.1. namely Isothermal Isobaric CVI (ICVI), Isothermal Forced Flow CVI (FCVI), Thermal gradient CVI (TGCVI), Thermal gradient Forced Flow CVI (TGFCVI), Pulsed CVI (PCVI) and Microwave assisted CVI (MWCVI). In ICVI; the gaseous reactants are transported into the porous preform (heated to constant temperature) via diffusion and deposit the solid matrix after the decomposition/chemical reaction. In this process, the process is made slow with less efficiency to minimize the over coating and to have uniform and optimum infiltration. The process is interrupted for surface machining to open up the closed pores to increase the infiltration rate and uniformity. Longer densification time (>400 hr) is required to achieve the required density. In FCVI process, the reactants are forced through the preform to increase the infiltration rate [8].

The temperature gradient was created in the preform and gaseous reactants are transported into the preform via chemical diffusion in TGCVI process to increase the infiltration rate. The infiltrations are started with hotter region of preform and proceed towards colder region of the preform and thereby increase the uniformity and minimize the canning. This method is very effective for small products having regular cross sectional geometry. In TGFCVI process, in addition to thermal gradient, across the preform, the gaseous reactants are forced through the preform to have uniform and increased infiltration rate.

In the microwave CVI, the preform is heated using microwave energy. If the preform is not microwave absorbent in nature, it is seeded with the susceptor to heat the preform. Since the microwave heating is volumetric heating and heat transfer is inside out, uniform and enhanced infiltration are achieved.

In the Pulsed CVI [9-11], the reactor is evacuated; reactant gases are sent into the reactor and allowed to react. After the reaction, the by-products are pumped out. This procedure is repeated till the required density is obtained. The above said CVI processes have their own advantages and disadvantages.Various precursor systems like (i) Methane (CH_4)- Silicon Tetrachloride ($SiCl_4$), (ii) Methyl trichloro Silane- MTS (CH_3SiCl_3)- Hydrogen (H_2) and (iii) Dimethyl Dichloro Silane [$(CH_3)_2$ $SiCl_2$]- Hydrogen (H_2) are used to derive CVD/CVI Silicon Carbide [9-16]. The advantage of MTS over other precursors is that Carbon and Silicon are present in the ratio of 1:1 to form stoichiometric SiC. It also exists in liquid form at room temperature with high vapour pressure and it can be evaporated and transported to the reactor using hydrogen as a carrier gas through Mass Flow Meter. The ICVI is the one which is commercially preferred, since it could be used to make large, complex and irregular geometries. The present study is focused on the preparation of C_f-SiC and SiC_f-SiC composites through ICVI process, the kinetic study to arrive an appropriate reaction temperature for a given molar flow rate ratio of hydrogen to MTS/pressure and various characterizations like physical (density and porosity), mechanical (flexural strength, RT tensile strength and fracture toughness) and SEM microstructure.

2. Experimental procedure

2.1. Sample Preparation

The Carbon cloth (8H satin) and Silicon Carbide cloth (8H satin CG Nicalon) are cut into required dimensions 118mm(L)x108mm(B) and the cut pieces are laid up to form respective C and SiC preforms. These preforms are loaded and compressed to the required level with the help of high temperature fasteners (CFC struts and nuts) in the perforated graphite tool having the cavity with the dimensions 120mm(L)x110mm(B)x4mm(H). The fibre volume fraction (V_f) is maintained around 40% in both C and SiC preforms.

2.1.1. SiC CVI Kinetic experiment

SiC preform having the dimensions of 120mm (L) X 50mm (B) X 4mm (H) with V_f of around 40% is held in the perforated graphite tool. The tool is then placed in an ICVI reactor (M/s Archer Technicoat Ltd, UK) chamber and SiC CVI is carried out using the MTS(99%, M/s. Spectrochem, India)/H_2 (99.995%, M/s. Inox air products Ltd, India) precursor system for 5 hour at various temperatures (950 °C, 970°C, 990°C, 1010°C and 1100°C) with the fixed pressure of 1.65mBar and molar flow rate ratio of 1:16. The reactor is evacuated and heated at slow rate (3-

4°C/min) with Ar purging. Once the temperature has reached the set value (950 °C-1100°C), it is stabilized for 10-20min. MTS precursor is metered through a liquid mass flow meter (M/s. Bronkhorst, Netherlands), vapourised in the evaporator and mixed with H_2 in the mixing chamber. The MTS/H_2 mixture is then entered into the reactor and MTS is cracked and solid SiC is formed on to the individual fibre and then fibre bundle. The weight gain in the preform is measured and recorded. The plot is made by taking 1/T (K^{-1}) along X axis and ln (Infiltration rate = weight gain/time duration of infiltration) along Y axis and various reaction regions are identified. The limiting steps in the chemical vapour infiltration of SiC from MTS/H_2 mixture are found. The temperature scheme for CVI experiments to have uniform and increased infiltration rate is arrived from the plot (Arrhenius plot). Care is taken to have identical preforms and to ensure the same position in the reactor chamber for controlled CVI experiments. The schematic representation of the experimental setup used for this study is shown in fig. 2.

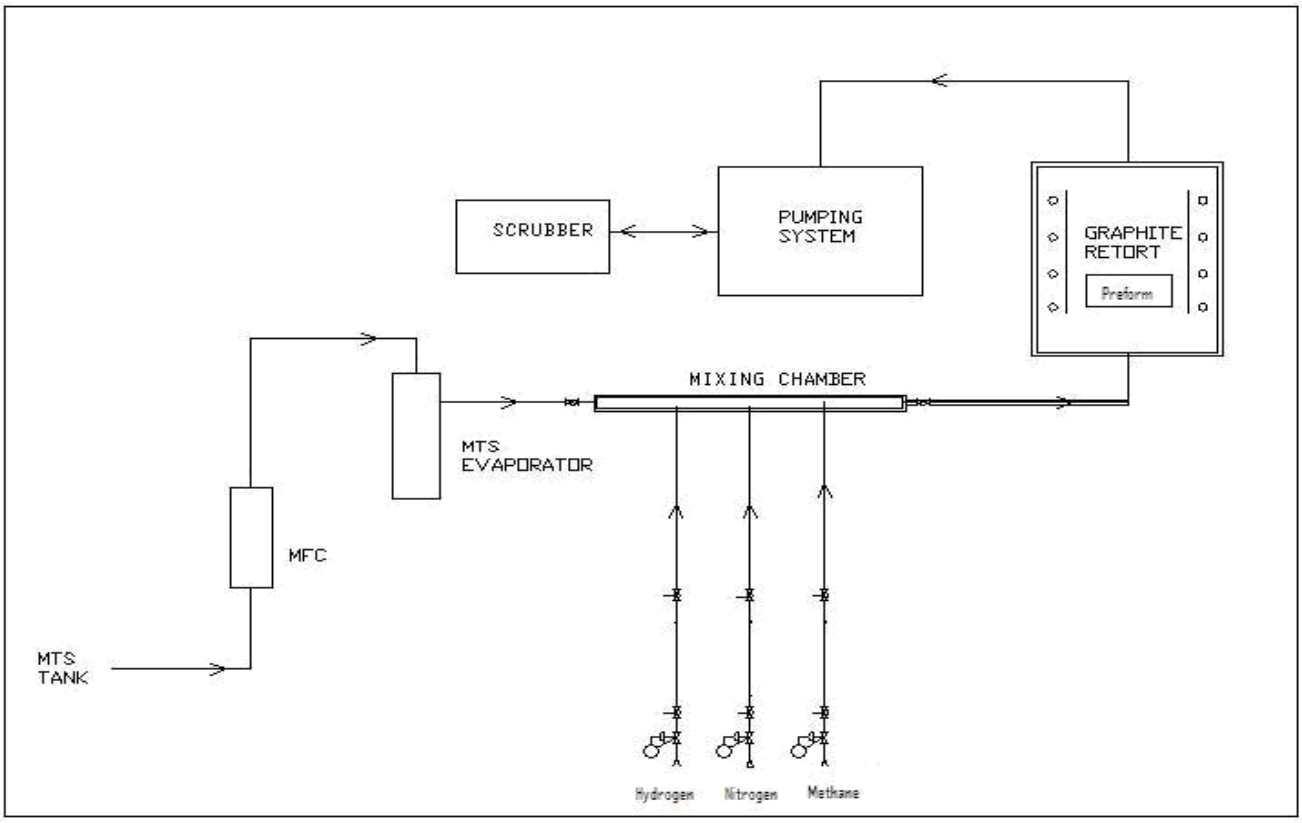

Figure 2 :- CVI experimental set-up

2.1.2. Preparation of C_f-SiC composites

The graphite tool holding the carbon preforms is loaded into the ICVI reactor. The reactor is evacuated and heated at slow rate (3-4°C/min) with N_2 purging. Once the temperature has reached the set value (1200°C), it is stabilized for 10-20min. CH_4 and N_2 gases are metered through a mass flow meter (M/s. Bronkhorst, Netherlands) and sent to the reactor to get the thin carbon interface

coating by cracking methane with the nitrogen as a dilution gas at a pressure of 1.6-1.7mBar to modify the interfacial bonding between fibre and matrix to improve the toughness [17-20]. The interface coating thickness is controlled by carrying out the C- CVI for known time (5hr, 10hr etc) to have two thicknesses. After the interface coating, the SiC-CVI is carried out to form CVI-SiC matrix by cracking MTS in the presence of H_2 as a catalyst cum carrier gas at the temperature range of 950°C-980°C and a pressure of about 1.65mBar. The molar flow rate ratio of MTS: H_2 used in this study is 1:16. Since the CVI is carried out in isothermal condition, it is obvious that the pores are getting closed through the phenomenon called canning. Hence, the multiple cycles of infiltration with intermediate surface machining to densify the preform to the required density is necessitated. The first few cycles are for bonding the cloth layers and rest of the cycles for densification. The total infiltration time required to get the density around 2.00g/cc is 500hr. C_f-SiC composites with 5 and 10 hr C interface are labeled as CQAV and CQAX. The first letter is for fibre type (C-Carbon fibre), second letter is for weave type (Q-satin) third letter is for interface type (A-Carbon) and fourth letter is for hours of interface coating (V-5hr and X-10hr).

2.1.3. Preparation of SiC_f-SiC composites

The graphite tool holding the SiC preform is loaded into the ICVI reactor. C interface is applied in the same way as mentioned in the section 2.1.2. BN interface is applied by the reaction between BCl_3

and NH_3 at a pressure of 1.6 mBar and a temperature of about 850°C. SiC matrix is obtained in the same way as mentioned in the section 2.1.2. C and BN interfaces are applied to have better mechanical properties [21-27]. SiC_f-SiC composites with C and BN interface are labeled as SQAV and SQBII. 850hr of SiC infiltration is carried out to achieve the density in the range 2.4-2.5g/cc. The first letter in the code indicates the fibre type (C for Carbon and S for SiC), second letter indicates the weave style (Q for satin), third letter stands for interface material type (A for C and B for BN) and last letter stands for hours of interface reaction. Typical graphite tool and SiC_f-SiC CMC panels are shown in fig 3a -3b.

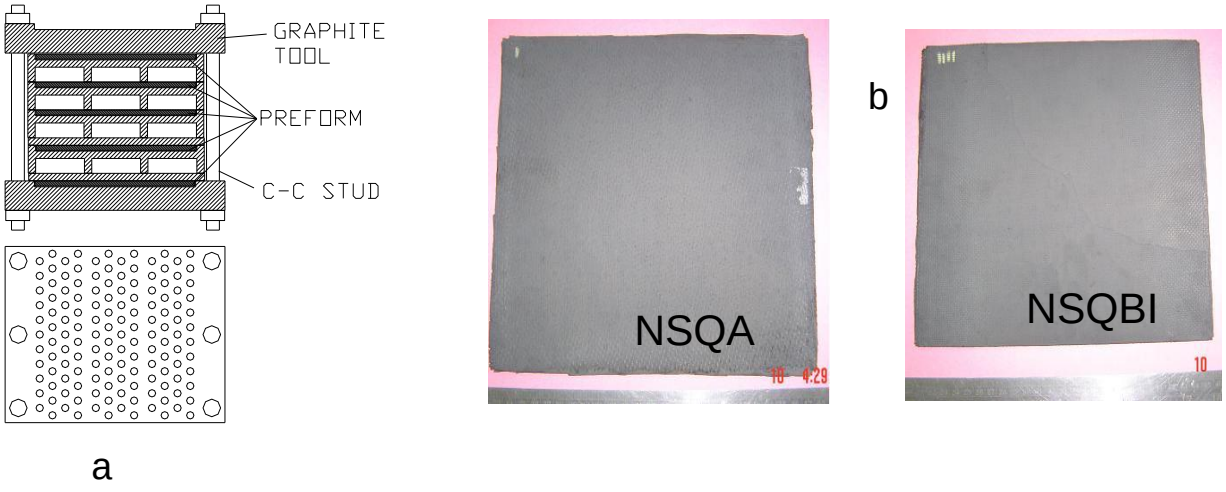

Fig.3a. Typical Graphite tool, 3b. SiC_f-SiC CMC panels(X and Y) with the dimensions L = 250mm X B=240mm X T=4mm.

2.2. Characterisation

2.2.1. Density and porosity measurements

The density and porosity of C_f-SiC and SiC_f -SiC composites are determined by Archimedes' method as per standard EN1389: 2003 [29].

2.2.2. X-ray diffraction studies

X-ray diffraction studies are carried out on prepared C_f-SiC and SiC_f -SiC composite samples to confirm the CVI derived matrix as β-SiC.

2.2.3. Mechanical Characterisation

C_f-SiC bar samples (length: 80mm x breadth: 6mm x thickness: 0.47mm) for flexural strength measurements are generated through water jet cutting from the prepared panels and tested using the universal testing machine (Instron model 1341 / 50 KN). The cut surfaces and edges of the samples are polished to remove the stress raisers. Room temperature (RT) flexural strength is measured by 4-point bending with the support span of 64mm and load span of 40mm as per the standard ASTM C1341 [30]. After the test, the side surface (length x thickness) of the bar is analysed under electron microscope (Leo 440i, M/s Leo UK) to find the failure mode and see how the crack propagated.

Sl No	Specimen/Test type	Dimensions (mm)
01	Bar specimen/Flexural strength (3 Point)	60(L)×6(W) ×4(Thick) for SiC_f-SiC 80mm(L) X 6mm(W) X 5mm(Thick) for C_f-SiC
02	Bar specimen/Fracture toughness	60(L)×6(W) ×4(Thick)
03	Dog bone specimen/Tensile strength	102(L), Gauge length-25, Width-6 and Thickess-4.

Table 1.0 Dimension details of the specimens used for various testing

SiC_f-SiC composites (SQAV and SQBII) specimens are generated for flexural strength, fracture toughness and tensile strength measurements through water jet with abrasive cutting. The dimensions and geometry of the specimens used for various tests are shown in table 1.0. The Room temperature (RT) flexural strengths are measured through 3 point bending method with a support span of 40mm and loading rate of 0.01mm/s using the universal testing machine (Bangalore Integrated Systems Solutions). RT tensile strength is measured using the Instron testing machine (model no: 5500J 7966) with a loading rate of 0.1mm/s. The SiC_f -SiC specimens are subjected to thermal exposure at 1000°C for 100hr in a furnace with oxidizing atmosphere and then their tensile strengths are measured to see the strength retention capability of the material. The SiC_f -SiC specimens (SQAV and SQBII) are also over coated with 60hr CVD SiC and their RT tensile strength is measured after subjecting them to thermal exposure (1000°C) for 100hr in a furnace with oxidizing atmosphere to see the effect of seal coating on strength retaining capability of composites.

All the faces of bar specimens (60mm X 8mm X 4mm) are polished down upto 1µ using diamond slurry to remove the stress raisers. The crack is created through thickness by cutting with 0.3mm thick diamond wheel. The crack is then sharpened by number of passes with a razor blade while irrigating the crack with 0.25 µ diamond suspension. The crack depth (a = 0.74mm) is measured [31] using the traveling microscope. These single edge notched specimens are loaded in 3point bending configuration and their breaking loads are measured. The K_{1C} values are measured using the following equation.

Fracture Toughness (K_{IC}) = $(3Pl/2bw^{3/2})$ X $[1.93 - 3.07(a/w) + 1.45(a/w)^2 - 25.07(a/w)^3 + 25.8(a/w)^4]$--(1)

Where P = load, L = span, b = thickness, w = width of the sample and a = crack depth.

2.2.4 Micro structural Characterization and Surface Analysis

SiC_f-SiC composite (SQAV and SQBII) specimens are generated from the prepared panels and polished down upto 1µ using diamond slurry. The polished surface is analyzed using Scanning Electron Microscope (Leo 440i, M/s Leo, U.K.) to see the microstructure showing the porosity, fiber distribution and interface between the fiber and matrix. Fracture surfaces of the composite samples with and without thermal exposure, tested for Tensile strength at room temperature, are analyzed under scanning electron microscope to see the signatures of fracture processes (e.g. fiber pullout).

3.0 Results and Discussions

Density and Porosity of the prepared composites are measured as per the standard EN1389:2003 and their results are shown in Table 2.0.

Sl No	Sample	Density(g/cc)	Porosity(%)
01	CQAX	2.003	14.5
02	CQAV	1.99	12.05
03	SQAV	2.45	16.5
04	SQBII	2.43	17.3

Table:2 .0 Density and Porosity of C_f-SiC and SiC_f-SiC composites.

It is seen from the Table 2.0; the density of CQAX is more or less same as that of CQAV. The porosity of CQAX is also comparable to that of CQAV. The RT flexural strength (4 point bending) of CQAV & CQAX is shown in table 3.0.

Sl No	Sample	Flexural Strength (MPa)
01	CQAX	342.38
02	CQAV	322.87
03	SQAV	350
04	SQBII	142

Table. 3.0. RT flexural strength of C_f-SiC and SiC_f-SiC composites

It is found from the table 3.0 that the RT flexural strength of CQAX is higher than that of CQAV. This higher strength may be due to the higher value of interfacial bond strength between matrix and fibre. However, the detailed studies to find the effect of interface coating thickness and the interfacial bond strength between matrix and fibre on the RT and high temperature flexural

strength are yet to be made. The typical load Vs stroke curves for CQAX and CQAV are shown in Fig 4.0 A. The SEM microstructures of side surface (through thickness) of CQAV and CQAX composites after the flexural testing showing crack deflection, matrix cracking and fibre pullout is shown in fig.4.0 B. It is evidenced from the microstructure that the fracture processes are observed in both the composites.

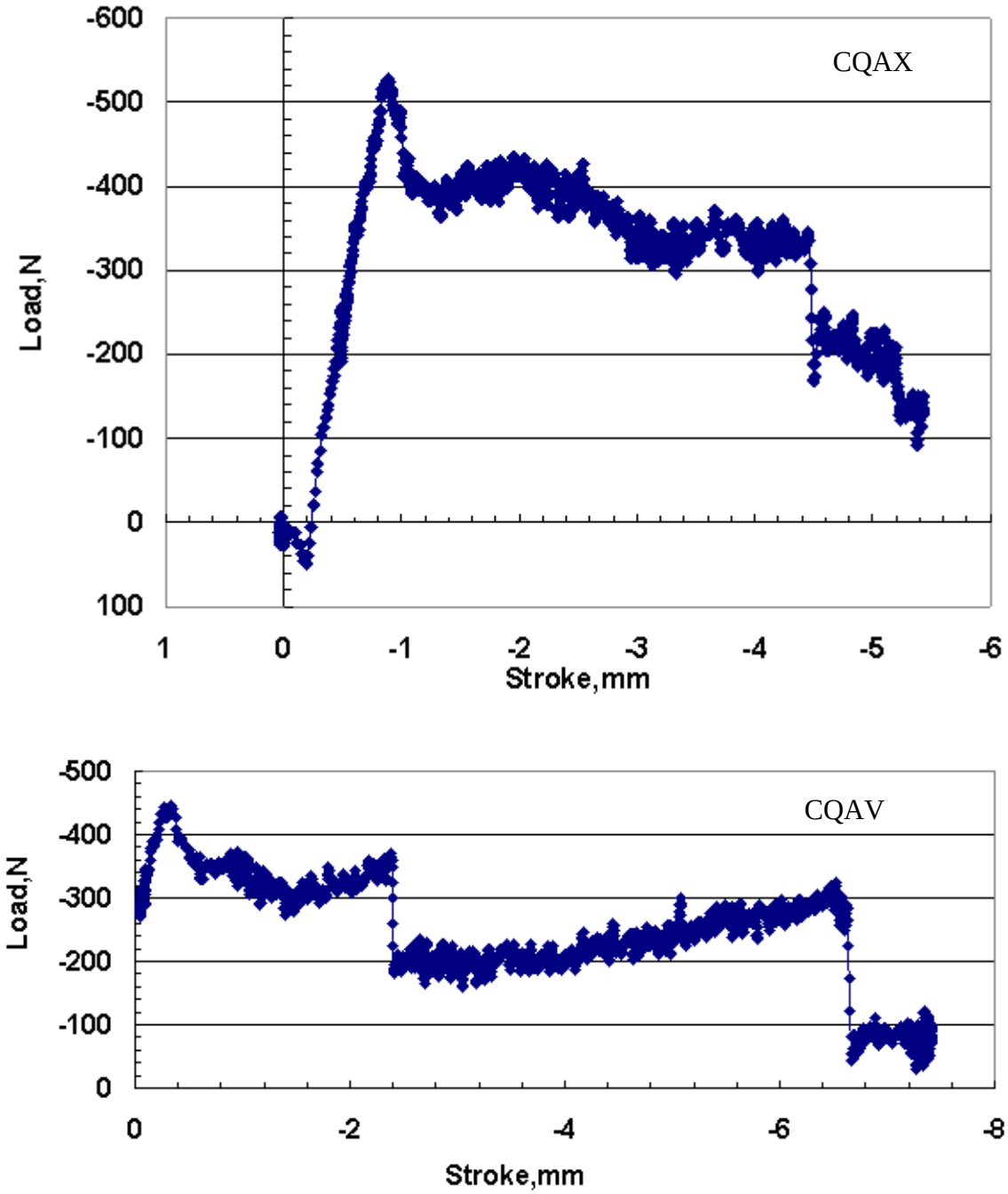

Fig. 4.0. A. Typical load vs stroke curve obtained for CQAX and CQAV.

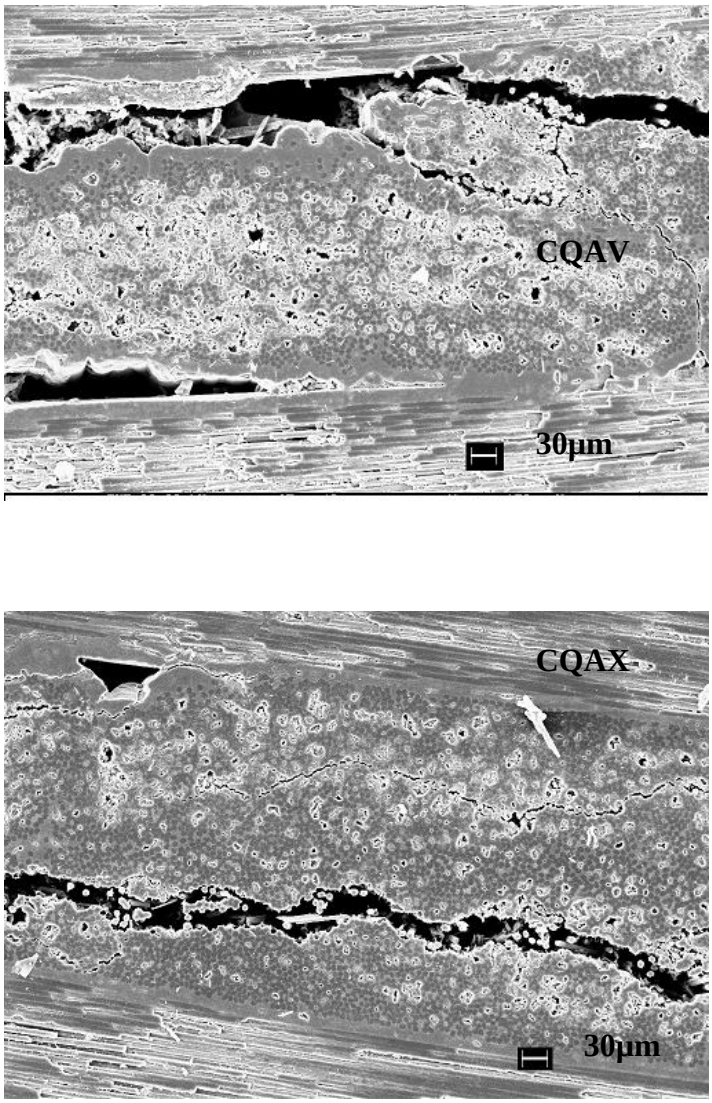

Fig. 4.0 B SEM Microstructures of side surface (through thickness) of CQAV and CQAX composites showing crack deflection, matrix cracking and fibre pullout.

The density and porosity results of SiC_f-SiC composites (SQAV and SQBII) are also shown in Table 2.0. The CVI process conditions (temperature 950^0C/ Pressure 1.65mBar and H_2: MTS=16:1) used are on the safe region and the products with uniform infiltration are obtained. However, longer hours of infiltration (80hr) are required to achieve the required density (2.4 - 2.5g/cc).

A widely used method to obtain CVD/CVI kinetic data is to determine the deposition/infiltration data experimentally as a function of process parameters (e.g. temperature, pressure, concentration of reactants etc.), and match them to the possible rate limiting reactions. A typical plot of infiltration rate as a function of temperature for SiC infiltration from MTS and H_2 is shown in fig .5.0. The plot complies with the Arrhenius law.

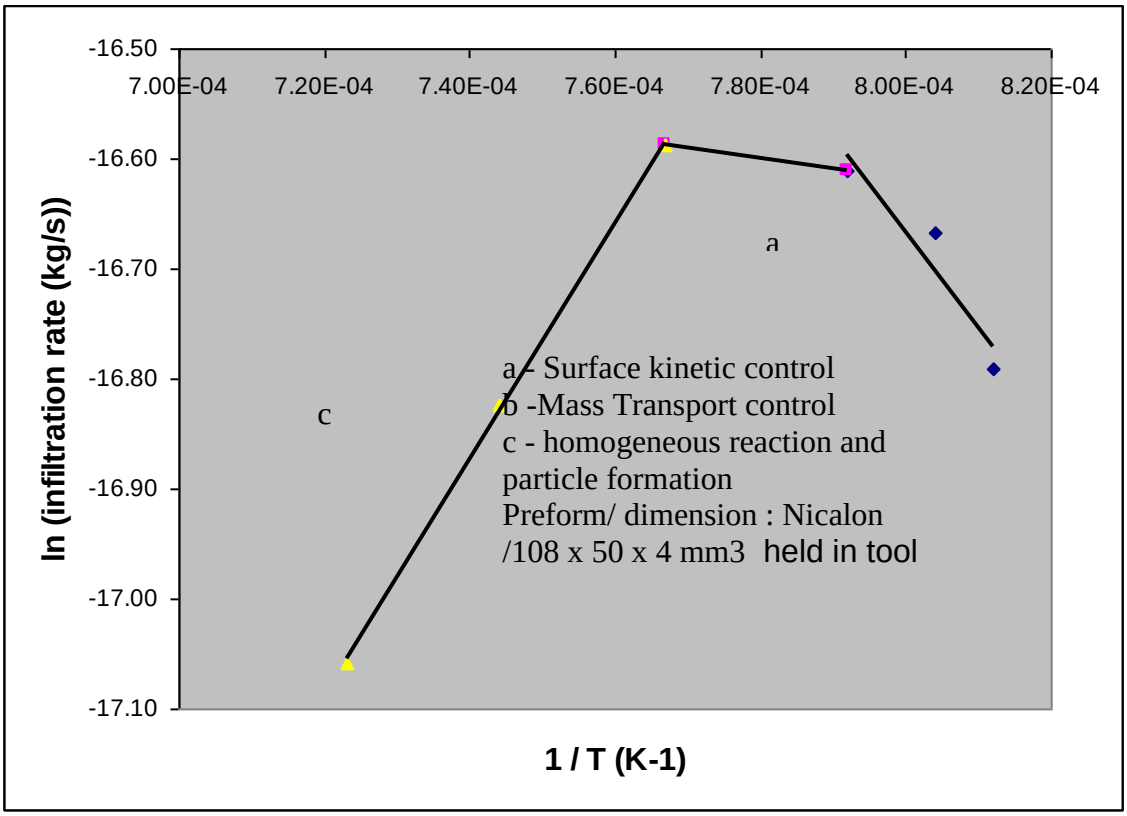

Fig. 5. 0. Arrhenius plot CVI of SiC from MTS/H_2

$$\text{Infiltration/deposition rate} = A\exp[-E_g/RT] \longrightarrow (2)$$

where A is a constant, E_g is apparent activation energy, R is the gas constant and T is temperature.

The plot shown in fig 5.0 indicates that three different reaction mechanisms are operating within the range of temperature (950^0C - 1110^0C) used, namely; region a-Surface kinetic control (950^0C to 990^0C), region b-mass transport control (upto 1030^0C) and region c-homogeneous reaction and particle formation. When the temperature increases from 950^0C to 990^0C (region a), the infiltration rate increases rapidly in an exponential manner. This indicates that the rate limiting mechanism is surface chemical kinetics: i.e., chemisorptions and/or chemical reaction, surface migration, lattice incorporation and desorption which are strongly dependent on the temperature. At higher temperature (990^0C - 1030^0C -region b), the surface kinetic process becomes such that the deposition is limited by the diffusion of active gaseous species through a boundary layer to the deposition surfaces. It is therefore mass transport limited, and the infiltration rate depends weakly on temperature. The transition from region 'a' to region 'b' seems to illustrate a classic transition of growth behaviour from interface control at low temperature to transport control at high temperature.

At even high temperature ($\geq 1090^0$C -region c), the infiltration rate is decreased. It is probably due to the depletion of reactants and/or increase in the rate of desorption. Other possible reasons for difference in slope may be due to the occurrence of alternate reaction involving high

temperature etching of SiC by corrosive reactant (CH_3SiCl_3) and by product (HCl) during the deposition of SiC.

SiC particle formation is also observed in the bottom of the CVI reactor chamber because of homogeneous reaction. From this simple kinetic study, it is suggested that the changing of reaction temperature (e.g. 950^0C as reaction temperature during the initial densification cycle, 970^0C as reaction temperature during middle of campaign and back to 950^0C towards the end of the densification period) as CVI campaign proceeds will speed up the infiltration than sticking to single temperature throughout the campaign (e.g. 950^0C). This scheme is followed in second CVI campaign and the total CVI process time is reduced by 30%. The details would be presented soon.

The X-ray diffraction results of the C_f-SiC and SiC_f-SiC composites are shown in fig 6 a-c. All the peaks are identified and they correspond to β-SiC phase. The peaks corresponding to C or Si are not observed. From the XRD results, it is evidenced that the process conditions used in this study yielded the required β-SiC phase and not the free C or Si.

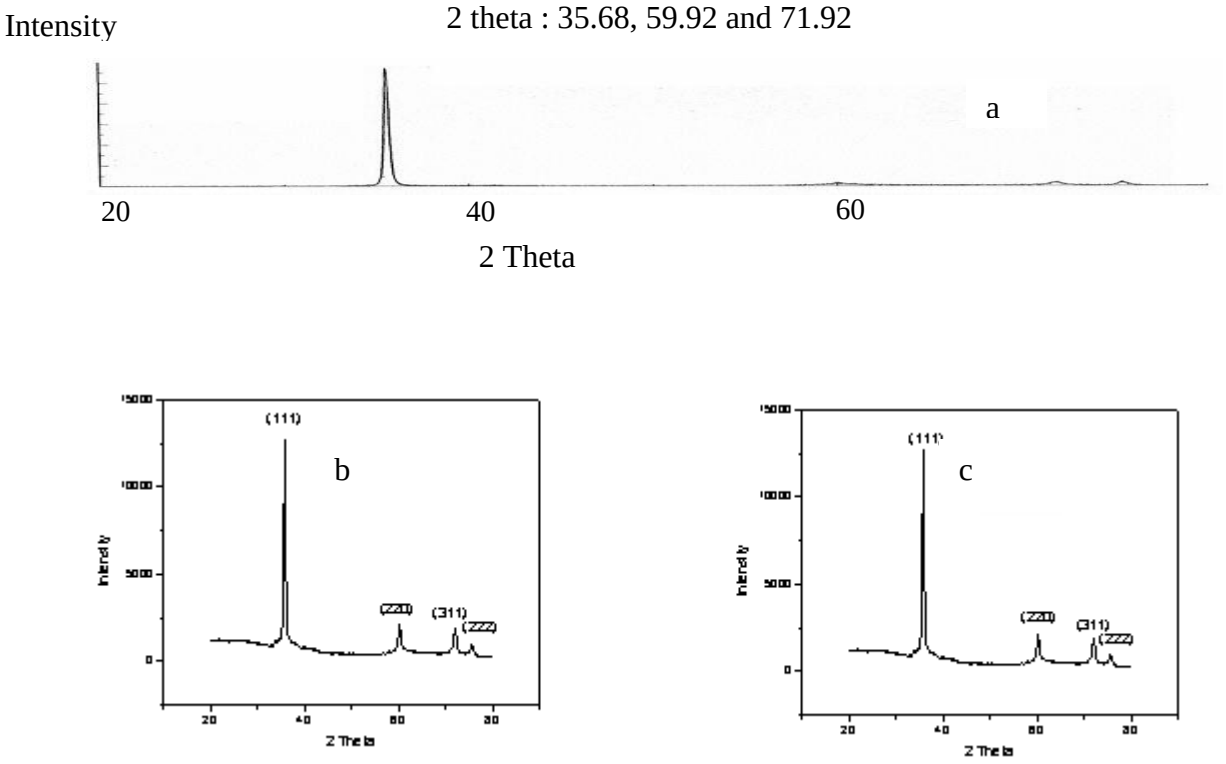

Fig. 6.0. X-Ray diffraction pattern for the composites a. C_f-SiC, b. SQAV and c. SQBII

RT tensile strengths obtained for the 2D-SiC_f-SiC (SQAV and SQBII) composite coupons with / without thermal exposure in oxidizing atmosphere at 1000ºC for 100 hr and with SiC seal coat followed by thermal exposure in oxidizing atmosphere are shown in table. 4.0. From the table.

4.0, it is found that average RT tensile strength of SQAV composite is 206 MPa which is matching with the literature values [32-33] whereas the RT tensile strength of SQBII is surprisingly low (68 MPa). The very low value obtained for SQBII is probably due to the unstable nature of BN as CVD coated at 850°C. The BN might have eaten away by moisture during many operations like water jet cutting, during unloading & reloading into the reactor and Archimedes' density measurements. It is suggested that as CVD coated BN is to be heat treated at atleast 1200°C in Argon atmosphere for 5 hr to have stable BN.

Sl No	Sample ID	Tensile strength(MPa)		
		RT without thermal exposure	**After thermal exposure at 1000°C/100hr and without seal SiC coat**	**After thermal exposure at 1000°C/100hr with seal SiC coat**
01	SQAV	206	57	201
02	SQBII	68	55	66

Table: 4.0.. Tensile results obtained on SiC_f-SiC (SQAV and SQBII)Composites

It is also found from the table 4.0, that the average RT tensile strength of SQAV composites without SiC seal coat and with thermal exposure in oxidizing atmosphere at 1000°C for 100 hr is only 57MPa which is 28% of its original strength. This reduction in strength is due to the fact that the C interface is oxidized and the SiC fiber got damaged during the thermal exposure as generated composite specimen without SiC seal coat is having plenty of pathways to oxygen as expected.

Whereas, the strength retention capability of SQBII is better (retained 69% of original strength) than SQAV. The 30% loss of strength is probably due to the further damage by the thermal exposure because of unstable nature of CVD coated BN. It is suggested to heat treat the CVD coated BN as mentioned above. The SiC seal coat on both the composites has really improved the strength retention capability of the material even after the thermal exposure as shown in the table. 4.0.

The typical load vs displacement curves obtained during the RT tensile strength measurements for both the composites (SQAV and SQBII) with different treatment and (with and without thermal exposure/SiC seal coat) are shown in fig..7a-c and fig. 8 a-c. It is evidenced from the fig. 7.a that SQAV composite without the thermal exposure exhibited a graceful failure where as the same exhibited brittle failure after thermal exposure (7b). This is because of fiber degradation, once the C interface is oxidized. The same composite with SiC seal coat failed in a non-catastrophic manner even after thermal exposure.

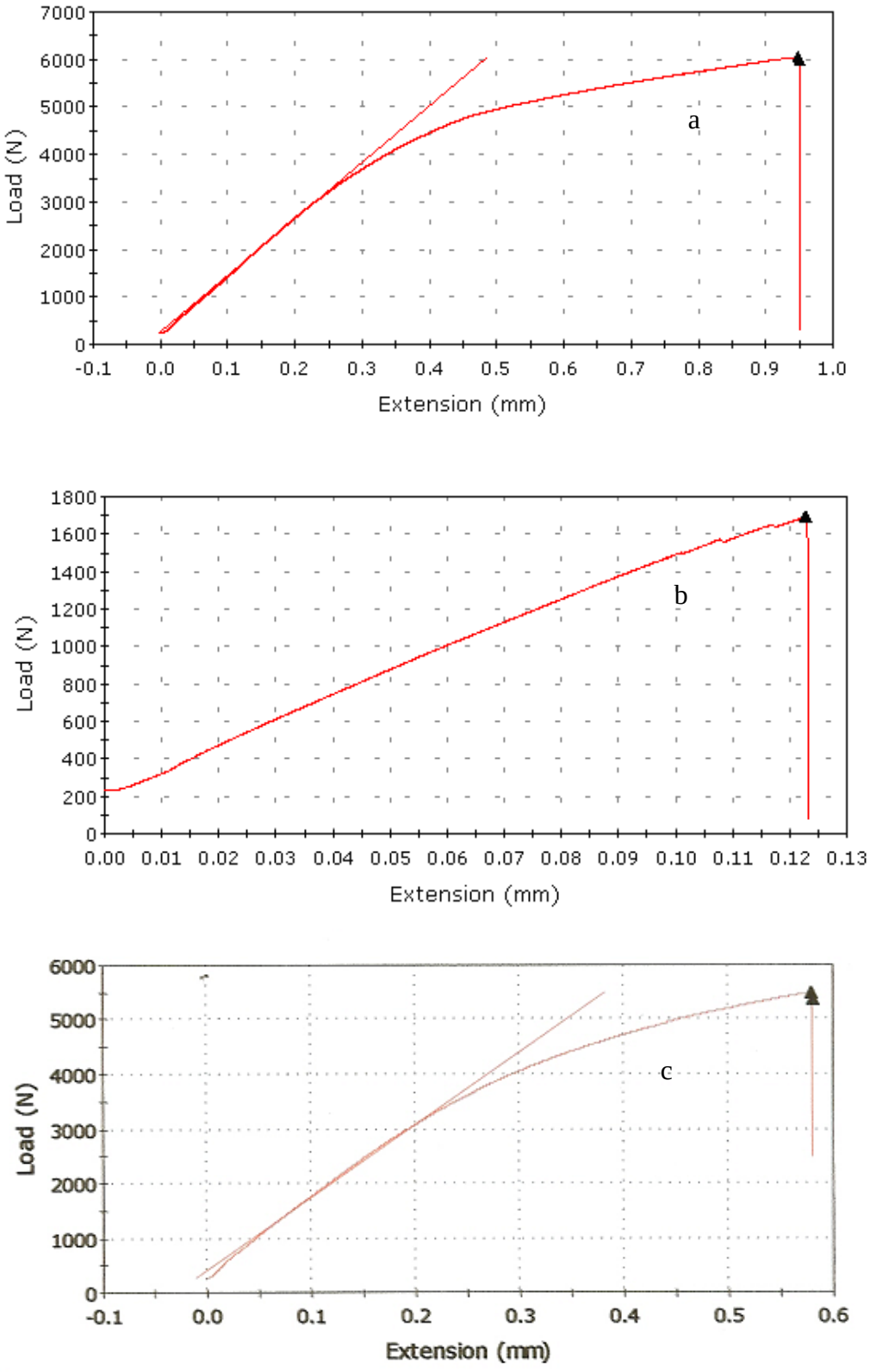

Fig. 7.0. Load Vs Displacement curve for SQAV composites a. without thermal exposure, b. with thermal exposure at 1000ºC for 100hr in oxidizing atmosphere and c. with SiC seal coat and thermal exposure at 1000ºC for 100hr in oxidizing atmosphere.

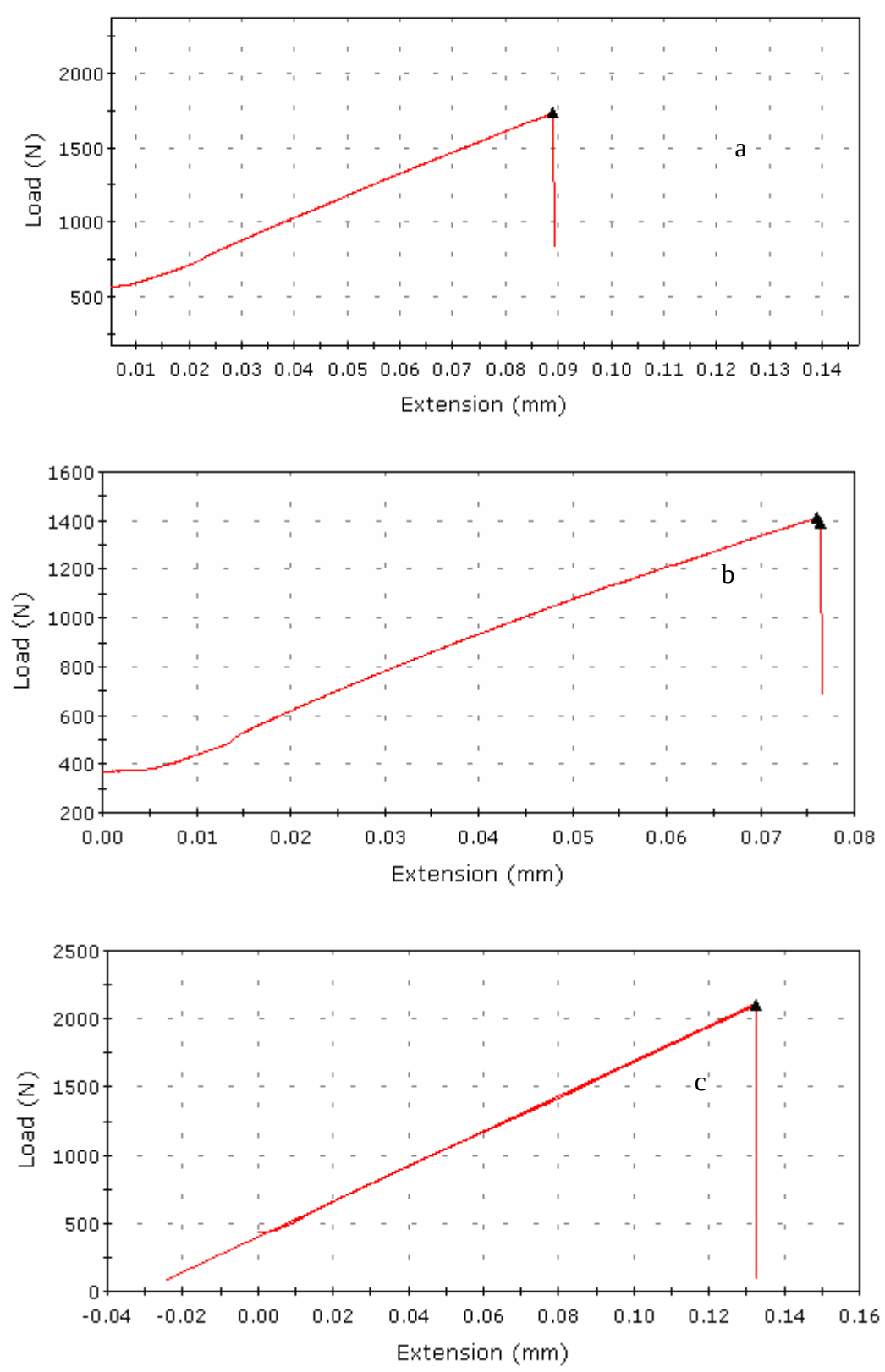

Fig 8.0. Load Vs Displacement curve for SQBII composites a. without thermal exposure b. with thermal exposure at 1000°C for 100 hr in oxidizing atmosphere and c. with SiC seal coat and thermal exposure at 1000°C for 100 hr in oxidizing atmosphere.

SQBII composite failed in a brittle manner in all the cases as seen in fig. 8a-c. This is due to the fact that, the BN is eaten away by moisture and further degraded during the thermal exposure. Hence, low strength is observed.

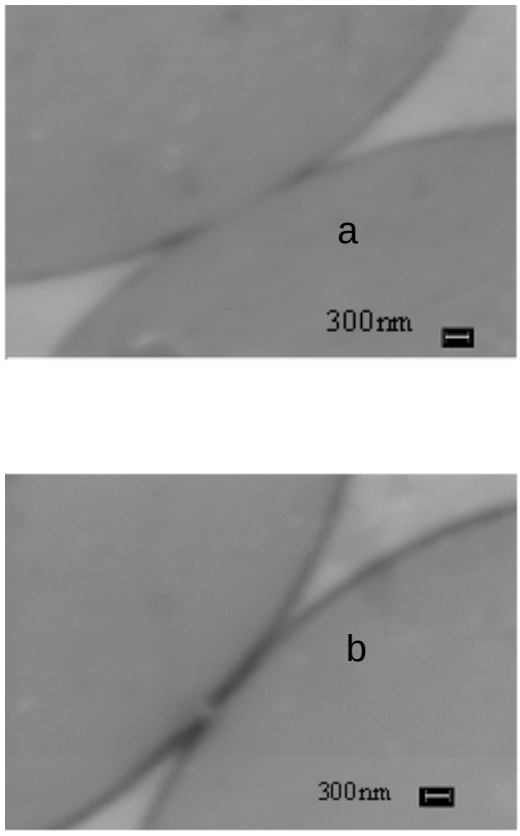

Fig. 9.0. SEM microstructure of a-SQAV and b-SQBII composites showing the fibre/matrix interface.

The SEM microstructure of SQAV and SQBII composites is shown in Fig. 9a-b. From the microstructure, it is seen that the C interface between fiber and matrix is thin (~90nm) and uniform. Whereas, the BN interface (150nm) is eaten away by the moisture. The low strength observed in the case of SQBII is may be due to poor load transfer. SEM microstructure of fractured surfaces of SQAV and SQBII composite samples after tensile testing is shown in fig. 10 and 11. Extensive fiber pull out is observed for the sample that shows graceful failure as evidenced in the microstructure fig.10a. It is noted that there is no fiber pull out in the case of SQAV composite without SiC seal coat after thermal exposure. It is may be because of the oxidation of C interface. In the case of the same composite with SiC seal coat subjected to thermal exposure, the fiber pull out is observed, showing that the C interface is protected by the SiC seal coat.

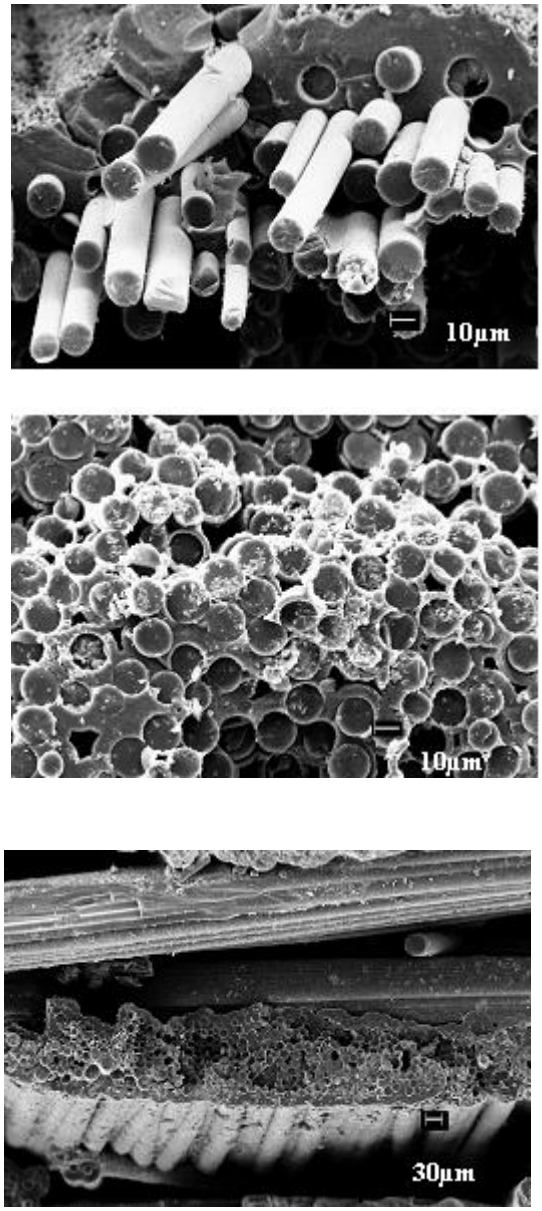

Fig. 10.0. SEM microstructure of Fracture surface (after RT tensile strength) of SQAV composites a - without thermal exposure in oxidizing atmosphere at 1000ºC for 100 hr showing fibre pull out and b & c - with thermal exposure in oxidizing atmosphere at 1000ºC for 100 hr showing less fibre pull out, oxidation of C interface and some silica formation i.e. cleavage fracture.

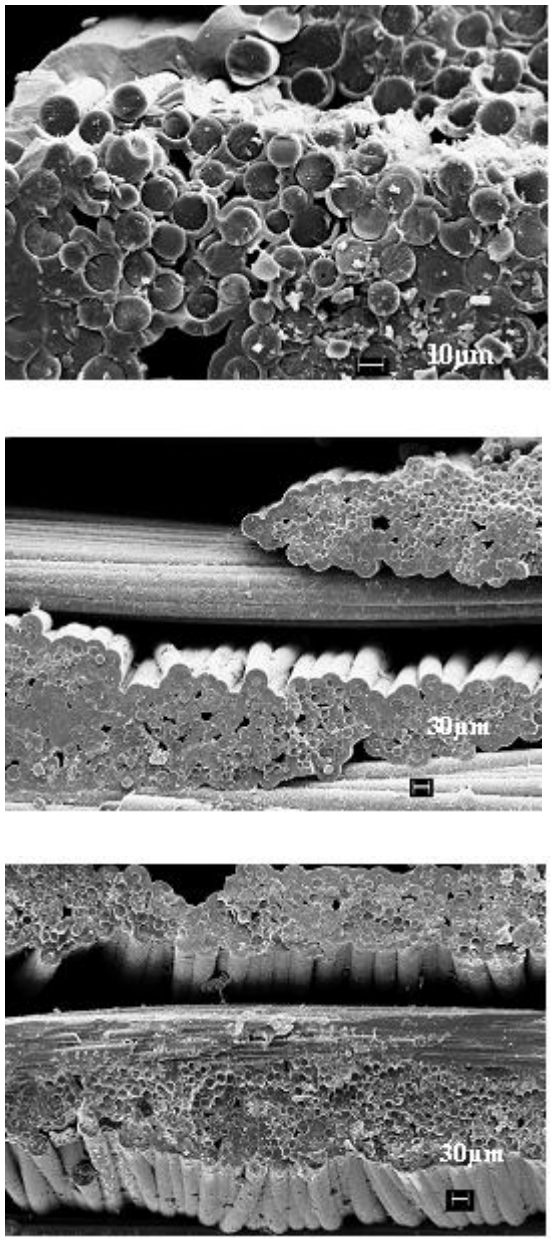

Fig. 11.0. SEM microstructure of Fracture surface (after RT tensile strength) of SQBII composites a - without thermal exposure in oxidizing atmosphere at 1000ºC for 100 hr showing no extensive fibre pull out and b & c - with thermal exposure in oxidizing atmosphere at 1000ºC for 100 hr showing less fibre pull out, delaminating, oxidation of C interface and some silica formation i.e. cleavage fracture.

For the SQBII composite, there is no fiber pull out in all the cases as seen in the fig. 11a-c. It confirms the brittle failure as seen in load vs displacement curve shown in fig. 8a-c. The flexural strength results (shown in table. 3.0 and fig. 12.0.) supports that the SQAV composites are tougher than the SQBII composites. From the load vs displacement curve (shown in fig.12.0.) obtained for both SQAV and SQBII through 3 point bending test, it is seen that SQAV exhibited a gradual failure compared to SQBII.

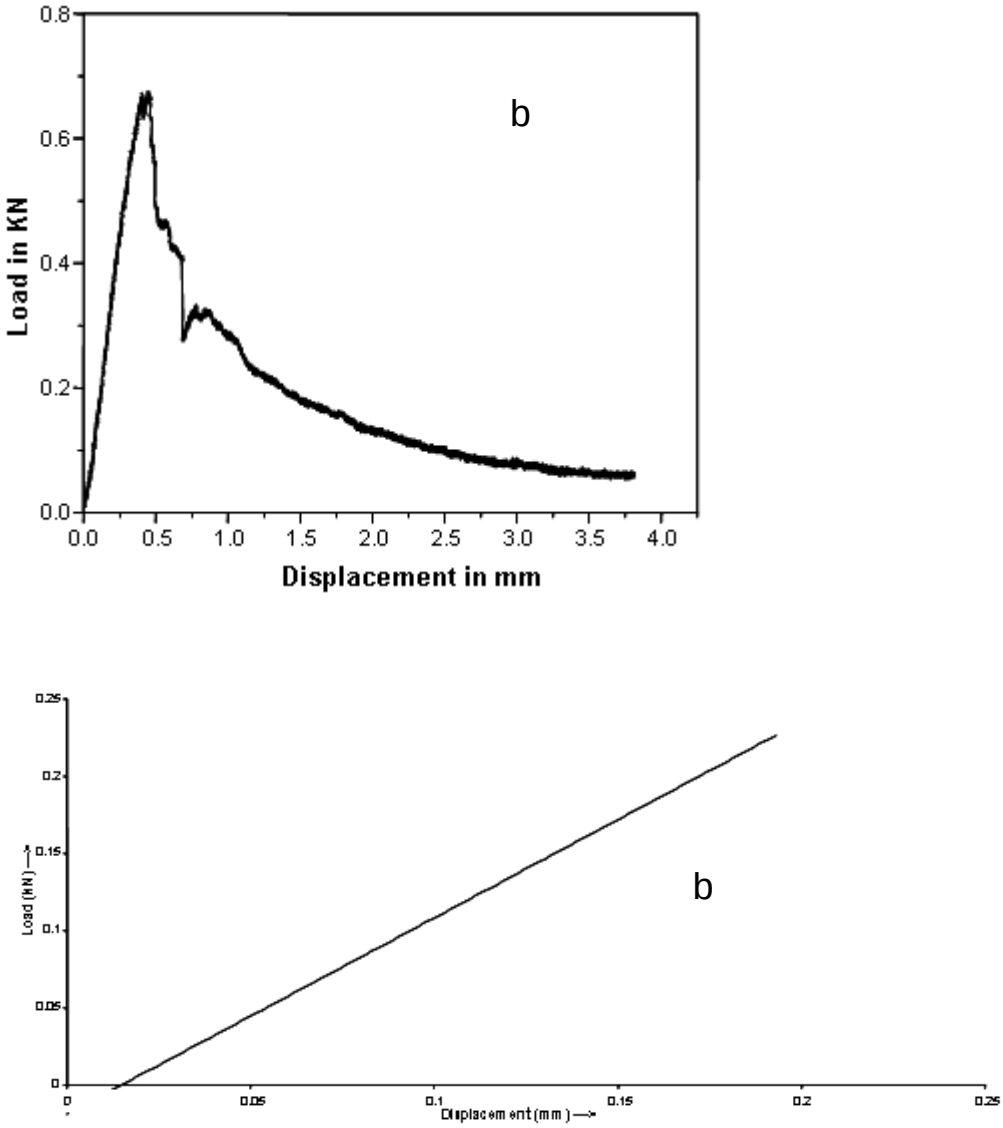

Fig. 12.0. Load Vs Displacement curves for a - SQAV composites and b - SQBII composites.

Fracture toughness (K_{1C}) of the SQAV composite is 36 MPa√m which is nine times that of typical monolithic SiC ceramics (4MPa√m) and K_{1C} of the SQBII composite is 16MPa√m. From the fig 13.a, it is evidenced that there is a good amount of fracture processes (matrix cracking, debonding, fiber sliding, crack bridging and fiber pull out) in the case of SQAV composite. In the case of SQBII composite, the failure was sudden and exhibited the cleavage fracture. This behavior of both the composites is clearly noticed in tensile strength, flexural strength and fracture surface analysis results.

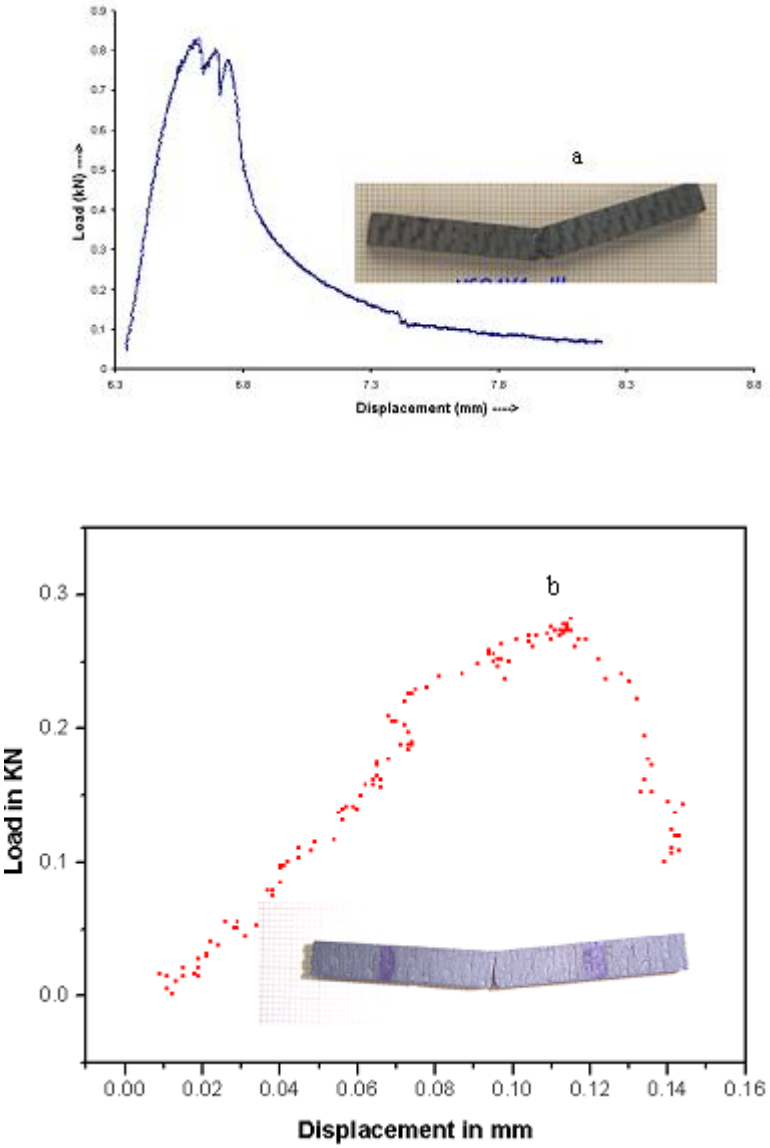

Fig. 13.0 . Load vs Displacement curve for a-SQAV Composites and b-SQBII composites obtained after K_{IC} test form 3 point bend test.

4.0. Conclusion

2D C_f-SiC and SiC_f-SiC composites were prepared through Isothermal Chemical Vapour Infiltration process. The density obtained for C_f-SiC composites was 2.0 g/cc. The density achieved for SiC_f-SiC composites was 2.4-2.5 g/cc after 850hr of SiC infiltration. The C and BN interface were applied to act as a mechanical fuse to have tougher SiC_f-SiC composites. The optimum CVI process temperature to get increased SiC infiltration rate with uniform density was obtained by simple kinetic experiment. CVI temperature scheme (changing the process temperature as CVI campaign proceeds) obtained from kinetic experiment results were followed in the second CVI campaign and 30% reduction in total process time was observed. The flexural strength of C_f-SiC was 342MPa. All the properties (tensile strength, flexural strength and K_{1C}) of SiC_f-SiC composite with C interface were better than SiC_f-SiC composite with the BN interface. It is suggested that as

CVD coated BN interface needs to be heat treated (at atleast 1200ºC for 5hr in Ar atmosphere) and stabilized the phase to retain the interface and have the advantage of BN interface to get the tough composites. The fracture toughness (K_{1C}) of SQAV composite is 36MPa√m which is nine times that of monolithic SiC ceramics (4MPa√m). The SiC seal coat has improved the strength retention capability of SQAV even after the thermal exposure at 1000ºC for 100hr in oxidizing atmosphere. Studies on SiC_f-SiC composite with BN interface (stabilized by the heat treatment) are currently going and results would be presented soon.

Acknowledgements

The authors thank Mr.M.A.Venkataswamy and team for the SEM studies, Mr. Manjunath and Mr.A.Sri Ganesh for mechanical characterization and Mr.P.Kumara, Mr.S.Ganesh, Ms.J.Revathi, Ms.K.Flora Edwina and Mr.M.Naveen for their helps in carrying out the experiments. The authors also thank the Director, NAL for his active support and constant encouragement. Financial support from DMRL is gratefully acknowledged.

References:-

[1] D.B.Marshall and A.G.Evans, Failure mechanisms in ceramic-fiber/ceramic matrix composites, J.Am.Ceram.Soc., 68 (1985) 225-231.

[2] A.G.Evans and D.B.Marshall, The mechanical bahaviour of ceramic matrix composites. Overview No. 85, Acta Metall., 37 (1989) 2567-2583.

[3] Starr TL. Ceram Eng Sci Proc1988:9:803.

[4] Bickardike RL, Brown ARG, Hughes G, Ranson H. Proc. 5th Conf. On Carbon. New York. Pergamon Press, 1962, p. 575.

[5] K.L. Choy, Chemical vapour deposition of coatings, Progress in Materials Science 48 (2003) 57-170.

[6] Lackey WJ. Ceram Eng Sci Proc. 1989;10;577.

[7] Stinton DP, Bessmann TM, Lowden RA, Am Ceram Soc Bull 1988;67;350.

[8] Y.G. Roman, D.P. Stinton and T.M. Vermann, Development of High density fibre reinforced Silicon carbide FCVI composites. Journal of Physique IV Collague C 2, Suppliau journal de physique II, Vol. 1 Sept. 1991

[9] Y.G. Roman, J.F.A.K. Kotte and M.H.J.M. de Croon, Analysis of the Isothermal Forced flow Chemical Vapour Infiltration process, Part I: theoretical aspects.

[10] S. Vaidyaraman, W.J. Lackey, P.K.Agarwal, G.V. Freeman and M.D. Langmann, Rapid processing of Carbon-Carbon composites by Forced flow thermal gradient Chemical Vapour Infiltration (FCVI). Mat. Res Soc symp. Proc. Vol 365 1995. Material Research Society

[11] Y. Ohzawa, H. Hoshino, M. Fuji Lawa, K. Nakane, K. Sujivama, Preparation of high temperature filter by pressure-pulsed chemical vapour infiltration of SiC into carbonized paper-fibre preforms. Journal of material science.

[12] H. Vincent*, C.Vincent, L. Oddou and T.S. Kannan. Chemically Vapour deposited coatings of silicon carbide on planar Alumina substrates.

[13] Jingyi Deng, Yengliang Wei and Wenchmess Liu, Carbon-fibre-reinforced composites with graded carbon-silicon carbide matrix composites. J. Am. Ceram. Soc, 82 (6) 1629-32 (1999)

[14] C. Vincent, J.P. Scharff, H.Vincent, J. Bouire, N. Lofti and T.S. Kannan. Chemical interation during the chemical vapour deposition of silicon carbide on Aluminosilicate fibres from halogenated precursors, Journal of Material Science, 29 (1994) 1-10

[15] David. P. Stinton, Theodore M, Besman and Richard A.Lowden, Advanced ceramics by chemical vapour deposition technique. J. Am. Ceram. Soc Bull 67 (2) Feb. 1998

[16] G.H.M. Gubbels, J.C.T. Vander Heijde, H.W. Brinkman, J.L. Linden and R.A. Terpetra. Development of ceramic components fore gas turbine application. Key Engineering Materials Vol 132-136 (1997) pp 2096-2099

[17] Cook. J and Gordon J.E (1964) Proc. R. Soc. London, A228, 508.

[18] T. Hinoki, W. Yang, T. Nozawa, T. Shibayama, Y. Katoh A. Kobyama.
Improvement of mechanical properties of SiC/SiC composites by various surface treatments of fibers. Journal of nuclear materials, 289(2001) 23-29.

[19] W.Jack Lackey, Sundar Vaidyaraman, Karren L. More, Laminated C-SiC matrix composites produced by CVI, J.Am.Ceram.Soc. 80 [1] 113-16 (1997)

[20] Ronald J. Kerans, Randall S. Hay, Triplicane A. Parthasarathy, and Michael K. Cinibulk, Interface design for oxidation-resistant ceramic composites, J.Am.Ceram.Soc., 85 [11] 2599-632 (2002)

[21] F. Lamouroux & G. Camus, Oxidation effects on the mechanical properties of 2D woven C/SiC composites, J. European Ceram.Soc. vol 14, No.2 (1994) 177-188

[22] N. Carrere, E, Martin, J. Lamon, The influence of the interphase and associated interfaces on the deflection of matrix cracks in ceramic matrix composites, Composites Part A 31 (200) 1179-1190

[23] H.C. Goo, E. Bischoff, O. Sbaizero, Manfred Ruhle and Anthony G. Evans, J. Am. Ceram. Soc, 73(6]1691-99(1990)

[24] Ken Goto, Yutaka Kagawa, Fracture behaviour and toughness of a plane-woven SiC fibre-reinforced SiC matrix composite, Material Science and Engineering A211 (1996) 72-81

[25] Christopher R. Jones, Charles H. Henager, Jr. and Russell H. Jones, Crack Bridging by SiC fibres during slow crack growth and the resultant fracture toughness of SiC/SiC_f composites, Acta Metallergica Inc. Vol.33, No.12 (1995) 2067-2072

[26] F. Rebillat, A Guette, L Espitalier, C. Debieuvre and R. Naslain, Oxidation resistance of SiC/SiC micro and mini composites with a highly cryatallised BN interphase, Journal of the European Ceramic Soc. 18 (1998) 1809-1819

[27] T. Hinoki, W. Zhang, A. Kohyama, S. Sato, T. Noda. Effect of fibre coating on interfacial shear strength of SiC/SiC by nano-indentation technique, Journal of Nuclear materials, 258-263 (1998) 1567-2571

[28] M. Leparoux, L. Vandenbulcke, V. Serin, J. Sevely, S. Goujard and C. Robin-Brosse, Oxidising environment influence on the mechanical properties and microstructure of 2D-SiC/BN/SiC composites processed by ICVI, Journal of the European Ceram. Soc., 18 (1998) 715-723

[29] European Standard EN 1389 : 2003, DIN EN 1389, Advanced technical ceramics, ceramic composites, physical properties-determination of density and apparent porosity, June 1994 edition

[30] ASTM C 1341, Standard test method for flexural properties of continuous fibre-reinforced advanced ceramic composites

[31] Yongdong Xu, Laifei Cheng, Litong Zhang, Hongfeng Yin, Xiaowei Yin, High toughness, 3D textile, SiC/SiC composites by CVI, Material Science and engineering A318 (2001) 183-188

[32] Lacombe, A. and Rouges, J.M. (1990) in AIAA'90, Space program and technologies conference '90, Huntsville, Al, September, 1990. Am. Inst. of Aero. and Astro., Washington DC, AIAA-90-3837.

[33] Lacombe, A and Bonnet, C. (1990) in AIAA'90, 2nd Int. Aerospace planes conference '90, Orlando, Fl, October, 1990, Am. Inst of Aero. and Astro., Washington, DC.